

In situ investigation of the selenization kinetics of Cu–Ga precursors using time-resolved high-temperature X-ray diffraction

W.K. Kim^a, E.A. Payzant^b, T.J. Anderson^{a,*}, O.D. Crisalle^a

^a Department of Chemical Engineering, University of Florida, Gainesville, FL 32611, USA

^b Materials Science and Technology Division, Oak Ridge National Laboratory, Oak Ridge, TN 37831, USA

Available online 19 December 2006

Abstract

In situ high-temperature X-ray diffraction was used to investigate the reaction mechanism and kinetics of CuGaSe₂ formation from Cu–Ga precursors during selenization. The precursor films were deposited in a migration enhanced molecular beam epitaxial reactor on Mo-coated thin glass substrates. During the selenization CuSe forms in the temperature range of approximately 260 to 370 °C, and the onset of formation of CuGaSe₂ occurred at approximately 300 °C. The kinetic analysis using a modified Avrami model suggests the formation of CuGaSe₂ from selenization of Cu–Ga films follows a one-dimensional diffusion-controlled reaction with an apparent activation energy of 109 (±7) kJ/mol. © 2006 Elsevier B.V. All rights reserved.

Keywords: X-ray diffraction; CuGaSe₂; Selenization; Avrami model

1. Introduction

Chalcopyrite Cu(InGa)Se₂ (CIGS) is a proven absorber material for high efficiency thin film solar cells with reported conversion efficiency of 19.5% using an In-rich absorber [1]. One approach to reach an even higher efficiency CIGS based-solar cell is the tandem cell structure that uses the high efficiency In-rich CIGS device as the bottom cell. CuGaSe₂ has a band gap energy of 1.68 eV, and thus is a promising absorber material for the top cell in a CIGS tandem solar cell structure [2–4]. Recently, a record-efficiency of 10.23% for a surface-modified single junction CuGaSe₂ cell was reported by NREL [5].

The commonly used approaches for CIGS layer formation are co-deposition of elements [6], rapid thermal processing (RTP) of stacked or co-deposited Cu/In/Ga/Se precursors [7,8], and selenization of metallic precursors in H₂Se or Se vapor [6,9]. A detailed understanding of the phase equilibria and formation kinetics of CIGS and its sub-ternaries would greatly assist the development of robust process models to optimize a high performance and cost-effective commercial process. While there have been several studies regarding the equilibrium phase diagram [10–12] and reaction mechanism [13–17] of CuInSe₂,

only a few fundamental investigations of the CGS system have been reported. Purwins et al. reported the formation of CuGaSe₂ from a stacked bilayer Ga₂Se₃/Cu₂Se followed a nucleation and growth model with an activation energy of 129 kJ/mol, which is extracted from a Kissinger analysis of differential scanning calorimetric data [18].

Our research group has conducted a systematic study of the reaction pathways and kinetics of formation of CIGS and its sub-ternaries (e.g., CuInSe₂ and CuGaSe₂) using *in situ* high-temperature XRD. In these studies, the reaction pathway and kinetics of α -CuInSe₂ formation from different precursors (e.g., InSe/CuSe and In₂Se₃/CuSe) and selenization of metallic Cu–In precursor have been presented [19–21]. In this paper, the reaction pathways and kinetics for CuGaSe₂ formation by the selenization of Cu–Ga/Mo/glass precursors are investigated using *in situ* time-resolved, high-temperature X-ray diffraction.

2. Experimental details

The Cu–Ga/Mo/glass precursor was prepared in a migration enhanced molecular beam epitaxial (MEE) reactor under ultra high vacuum conditions (10^{−7} to 10^{−8} Torr). Since molybdenum is a widely used back-contact material in CIGS-based solar cells, the elemental Cu and Ga were deposited on Mo-coated, sodium-free thin glass (Corning 7059; alkali level <0.3%,

* Corresponding author. Tel.: +1 352 392 0946; fax: +1 352 392 9673.

E-mail address: tim@ufl.edu (T.J. Anderson).

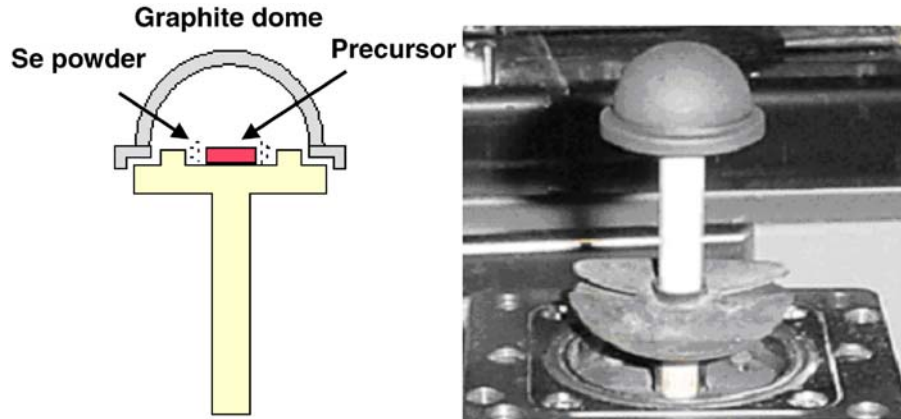


Fig. 1. X-ray sample holder with a graphite dome for selenization of Cu–Ga precursor films.

0.4 mm thickness) without heating the substrate to minimize the unintended reaction between Cu and Ga. The phase evolution and reaction kinetics during selenization of Cu–Ga/Mo/glass precursors were investigated using time-resolved *in situ* high-temperature X-ray diffraction (HT-XRD), which consists of a PANalytical X'Pert Pro MPD/X-ray diffractometer (Cu $K\alpha$ ($\lambda=1.54056$ Å) radiation source) equipped with an Anton Paar XRK-900 furnace and an X'Celerator solid state detector. Selenium powder was placed in wells on the HT-XRD sample holder adjacent to the precursor film. As shown in Fig. 1, the HT-XRD sample holder containing the precursor film and selenium powder was covered with an X-ray transparent graphite dome, which is customized to minimize Se vapor loss. The sample temperature in the HT-XRD chamber was calibrated from a determination of the lattice expansion of silver powder dispersed on an identical Mo-coated thin glass substrate. The silver lattice parameters could be converted to accurate sample temperatures based on the equation of linear thermal expansion as a function of temperature suggested by Touloukian [22].

3. Results and discussion

The overall atomic composition of the Cu–Ga film as-deposited on the Mo/glass substrate was measured as $[Cu]/[Ga]=1.01\pm 0.03$ by inductively coupled plasma optical emission spectroscopy (ICP-OES). The crystalline phases present in the as-grown precursor (mainly $CuGa_2$) and selenized film (mainly $CuGaSe_2$ and $MoSe_2$) were identified by room-temperature XRD (RT-XRD), as shown in Fig. 2. The thicknesses of the Mo (~ 0.4 μm), Cu–Ga (~ 0.7 μm), and selenized $CuGaSe_2$ (~ 1.2 μm) films were measured by SEM images of cleaved samples, which are not shown here.

The selenization reaction was thermally promoted via temperature-ramp annealing at a rate of around 20 °C/min under *in situ* XRD observation to identify the possible intermediate phases and the temperature range for formation of the $CuGaSe_2$. As shown in Fig. 3, the results reveal that $CuSe$ forms in the temperature range of approximately 260 to 370 °C, and that the onset of formation of $CuGaSe_2$ occurs at approximately 300 °C. A strong carbon (002) peak from the

graphite dome was consistently observed at around a 2θ value of 27°. Fortunately, this peak did not overlap with any peaks of the anticipated phases. It is also noted that the peak intensities are attenuated over the entire 2θ range in the temperature range 370 and 600 °C, which is attributed to the scattering of the incoming X-ray by Se vapor within the chamber. Thus the almost full recovery of peak intensities at 600 °C demonstrates the complete consumption of Se vapor at this temperature.

The formation of $MoSe_2$ identified in the RT-XRD scan for the selenized film, as shown in Fig. 2(b), was not detected under *in situ* HT-XRD observation during temperature-ramp annealing, which is attributed to the relatively low resolution at the higher scan rate of HT-XRD ($\sim 8^\circ/min$) than that of RT-XRD ($\sim 1^\circ/min$). There are several reports on $MoSe_2$ formation at the interface of CIGS and Mo layers and its positive contribution to the efficiency of CIGS solar cells [23–25]. Wada et al. reported that the (100) and (110) reflections of $MoSe_2$ in CIGS/Mo absorbers deposited by a typical three-stage process were detected by XRD. They suggested that the CIGS/Mo heterocontact with the $MoSe_2$ layer makes a favorable ohmic contact, while CIGS/Mo without a $MoSe_2$ layer exhibits a Schottky-type contact [23]. In our previous report on selenization of Cu–In/Mo/glass precursor [21], the production of $MoSe_2$ was only detected after complete formation of $\alpha-CuInSe_2$. $MoSe_2$ detection was also accompanied by a rapid decrease of the

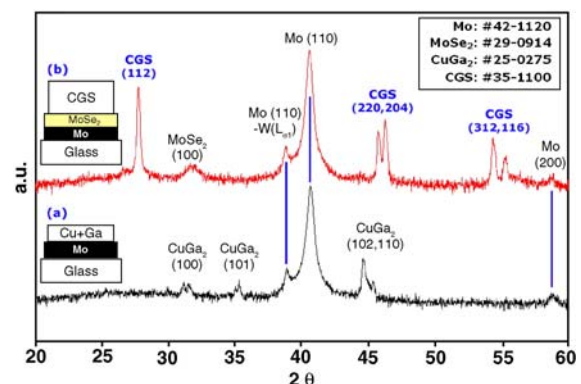


Fig. 2. Room-temperature XRD scans of (a) Cu–Ga as-grown precursor and (b) selenized $CuGaSe_2$ film.

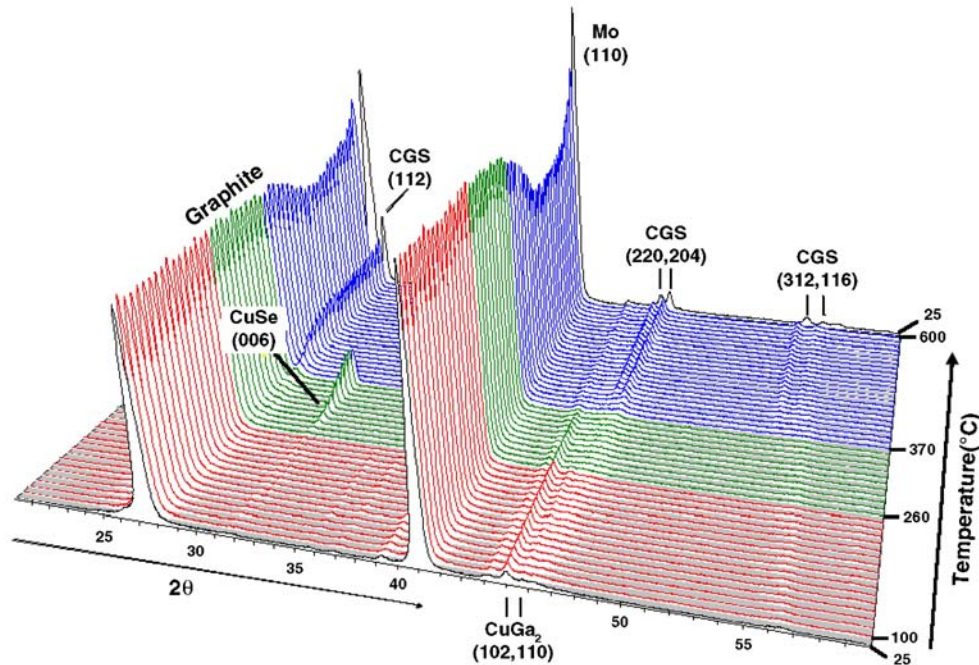


Fig. 3. *In situ* XRD scans during temperature-ramp selenization of Cu–Ga/Mo/glass precursor.

Mo (110) reflection intensity, which was clearly detected at a temperature above 440 °C. The greater thermodynamic stability of CIS over MoSe_2 is consistent with this observation.

Isothermal annealing at selected temperatures between 330 and 400 °C was then performed for estimating kinetic parameters using an appropriate reaction model. The 2θ scan range (22 to 30°) for the isothermal experiments was selected since the major reflection for the product CuGaSe_2 (112) lies within this range. To complete the reaction, the temperature was elevated to 550 °C after each run and then maintained at this temperature for about 12 min or until only the CuGaSe_2 phase remained as evidenced by constant peak intensity. Fig. 4 displays the time-resolved XRD data collected for the film isothermally annealed at different temperatures. The comparison between the isothermal plots at four different temperatures clearly illustrates that the reaction rate increases with temperature.

To obtain the fractional reaction (α), which is defined as the fraction of reaction completed at time t , the integrated intensities of the product CuGaSe_2 (112) peaks were obtained by fitting the diffraction data. The integrated intensities were then normalized assuming that the Cu–Ga precursors were completely selenized to crystalline CuGaSe_2 after the high-temperature anneal at the end of the run, and that the texture of the CuGaSe_2 did not appreciably change through the entire heating process. Although using the integrated intensity of fully reacted sample to estimate the fractional conversion is an approximation, the small sample thickness and the similar absorption coefficients of the precursor and CuGaSe_2 results in a relatively small error. A simple calculation on X-ray self-absorption with a precursor thickness 0.7 μm and a fully reacted thickness of 1.2 μm yields a maximum error from X-ray beam attenuation of less than 6% and this error decreases

as the reaction proceeds. This uncertainty should not affect the conclusions of the kinetic analysis.

The reaction kinetics in terms of an activation energy and reaction order were investigated using the Avrami model [19–21,26]. The Avrami model considers a reaction of the additive type between reactants, where the product phase is growing from randomly distributed nuclei within a reactant phase. Analysis of solid-state reaction data using the Avrami model is commonly used for preliminary identification of growth rate laws. Since isotropic growth is assumed in the Avrami model, the product regions should be spherical. The isothermal Avrami transformation rate with an initial condition of $\alpha(t=0)=0$ is given by

$$\alpha = 1 - \exp(-(kt)^n) \quad (1)$$

where α is the fractional reaction extent ($0 \leq \alpha \leq 1$), k is the Avrami kinetic rate constant, and n is the Avrami exponent.

According to the results of the isothermal experiments shown in Fig. 4, nucleation and partial growth of the CuGaSe_2 phase occurred during the heating period before the sample temperature reached the set-point, *i.e.*, $\alpha(t=0) \neq 0$. Considering this initial condition, a modified Avrami expression is suggested:

$$\alpha = 1 - \exp(-(k(t+t^*))^n) \quad (2)$$

or equivalently, as

$$\ln(-\ln(1-\alpha)) = n \ln(t+t^*) + n \ln k \quad (3)$$

where t^* is the time constant which satisfies the initial condition (*i.e.*, $\alpha(t=0)=\alpha_0$) at a given approach to the set-point temperature. The time t^* is the time the sample would have to be at the isothermal soak temperature for a fractional extent of

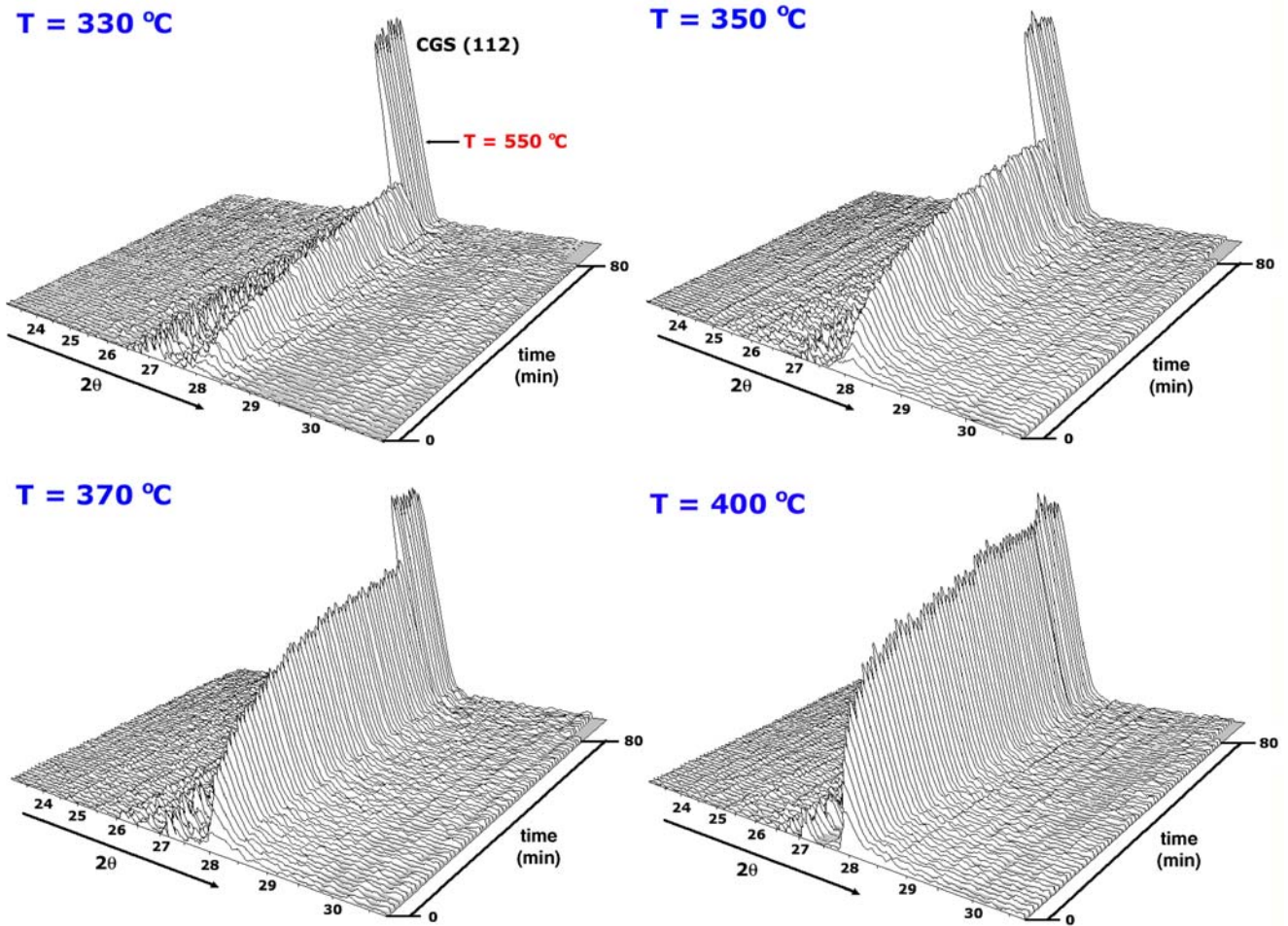


Fig. 4. *In situ* XRD scans during isothermal selenization of Cu–Ga/Mo/glass precursor at four different temperatures.

reaction to occur that is identical to that which actually occurs during the ramp to the anneal temperature. This time constant represents the starting time of reaction that is extrapolated from the Avrami model plot (*i.e.*, $\alpha(t=-t^*)=0$). To find the kinetic parameters, n , k and t^* , the following iteration steps are employed.

- 1) Guess the time constant t^* .
- 2) Find n and k by a multiple linear regression of the α vs. t data using Eq. (3)
- 3) Apply the initial condition, $\alpha(t=0)=\alpha_0$ to Eq. (3) to estimate the error, ε .

$$\ln(-\ln(1-\alpha_0)) - n \ln(t^*) - n \ln k = \varepsilon \quad (4)$$

The steps 1, 2 and 3 are repeated using the previous errors to estimate a new guess until an acceptable error (ε) is obtained.

In this analysis, the Avrami exponent (n) is known to vary between 0.5 and 1.5 in the case of one-dimensional, diffusion-controlled reactions [26]. The value of n is close to 0.5 if the nucleation is instantaneous, and close to 1.5 if the nucleation rate is finite and constant throughout the reaction. For our experimental data, the estimated Avrami exponents (n), kinetic constants (k), and time constants (t^*) are summarized in Table 1.

It is noted that the value of t^* increases with temperature, except at the two highest temperature in which the values are similar. This is expected given the longer time to temperature and average higher temperature during a ramp to a higher temperature. As shown in Fig. 5, the comparison between the fractional reaction by experiments and the prediction by a modified Avrami model demonstrates that a modified Avrami model fits the experimental data set very well. The n values over the entire temperature range (330 to 400 °C) lie in the relatively narrow range 0.55 and 0.61. These values are close to the lower limiting value of 0.5 thus suggesting rapid nucleation.

Table 1

Estimated kinetic parameters for the CuGaSe₂ formation from selenization of Cu–Ga/Mo/glass precursor films

Temperature [°C]	Modified Avrami model parameters		
	n	$k \times 10^3$ [s ⁻¹]	t^* [s]
330	0.57 ($\pm 1.5 \times 10^{-2}$)	0.302 ($\pm 1.63 \times 10^{-3}$)	0 ^a
350	0.55 ($\pm 1.1 \times 10^{-2}$)	0.703 ($\pm 2.27 \times 10^{-3}$)	38.6
370	0.61 ($\pm 1.7 \times 10^{-2}$)	1.38 ($\pm 7.71 \times 10^{-3}$)	62.0
400	0.61 ($\pm 2.8 \times 10^{-2}$)	2.92 ($\pm 4.26 \times 10^{-2}$)	54.3

(k : apparent kinetic constants, n : Avrami exponent and t^* : time constant of the modified Avrami model).

^a Experimentally determined since no pre-reaction was observed for this run.

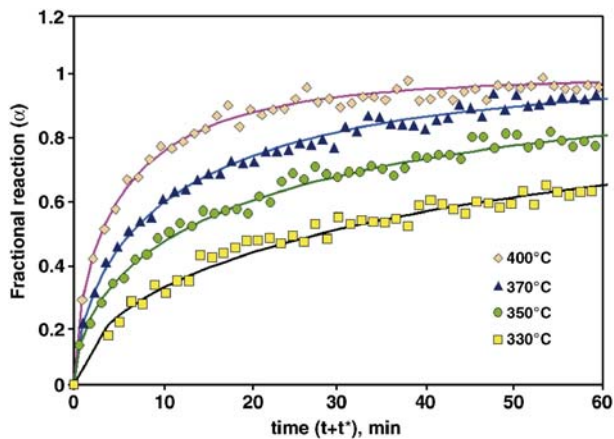


Fig. 5. Comparison of fractional reaction for isothermal experiments and modified Avrami model prediction. (Solid line: model predictions, symbol: experimental data).

The low value of the estimated Avrami exponents suggests that the nucleation of CuGaSe_2 occurs so rapidly (*e.g.*, during the ramping time) that the nucleation time is nearly negligible. The Arrhenius equation

$$k = A \cdot \exp\left(\frac{-E_a}{RT}\right) \quad (5)$$

was used to estimate the apparent activation energy, E_a , for CuGaSe_2 formation by selenization of Cu–Ga/Mo/glass precursor films. An activation energy of $109 (\pm 7)$ kJ/mol was estimated from the Arrhenius plot inserted in Fig. 6.

The value of $109 (\pm 7)$ kJ/mol is similar to the activation energy of $124 (\pm 19)$ kJ/mol estimated for selenization of Cu–In/Mo/glass precursor using the Avrami model and Arrhenius plot [21]. Also, this value is reasonably close to the activation energy of 129 kJ/mol estimated for CGS formation from the stacked bilayer $\text{Ga}_2\text{Se}_3/\text{Cu}_2\text{Se}$ by Purwins et al. [18]. It is interesting to compare the results of the formation of CGS to those of CuInSe_2 . Similar experiments using a Cu–In precursor showed a different reaction sequence (CuSe formation followed by CuSe_2 and then CuInSe_2). The analysis of the rate data by both the Avrami and parabolic rate models provided estimated activation energies of $124 (\pm 19)$ and $100 (\pm 14)$ kJ/mol, respectively, which are similar to the values determined here for CGS, suggesting the CuSe diffusion-controlled formation step may be rate limiting. It is also noted that from comparison of the standard errors of activation energies for CuGaSe_2 and CuInSe_2 formation by selenization of metallic precursors, it is concluded that the graphite dome used for selenization of Cu–Ga provides more reliable experimental results than the aluminum foil cover used for selenization of Cu–In. The experimental reliability of a graphite dome could be attributed to its superior X-ray transparency and operability compared to an aluminum foil. The X-ray transparency of the graphite dome is clearly evidenced by the negligible loss in reflection intensity, while employing an aluminum foil cover sacrifices the reflection intensity and thus the accuracy of experiments. Based on the results of the Avrami model analysis, the formation of CuGaSe_2 from selenization of Cu–Ga/Mo/glass precursor films apparently

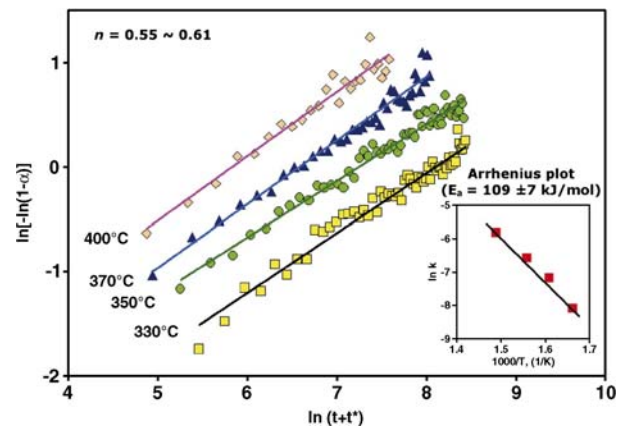


Fig. 6. Avrami model and corresponding Arrhenius plot (inset) for CuGaSe_2 formation by selenization of Cu–Ga/Mo/glass precursor.

follows a one-dimensional diffusion-controlled reaction with a nucleation and subsequent growth sequence.

4. Conclusions

The reaction pathway and chemical kinetics of CuGaSe_2 formation from Cu–Ga/Mo/glass precursor structures were investigated using time-resolved *in situ* high-temperature X-ray diffraction equipped with a graphite dome. The results show that the selenization process of Cu–Ga films produces a CuSe phase at temperatures ranging from 260 to 370 °C, and that CuGaSe_2 phase first starts to appear at approximately 300 °C. The kinetic analysis on the selenization of Cu–Ga films shows that a modified Avrami model for chemical reaction fits the experimental data set well, yielding an activation energy of $E_a = 109 (\pm 7)$ kJ/mol. This value of activation energy is very close to that estimated for the α - CuInSe_2 formation from selenization of Cu–In/Mo/glass precursor (*i.e.*, 124 ± 19 kJ/mol estimated with the Avrami model). It is concluded that the Cu–Ga selenization follows a pathway along a one-dimensional diffusion-controlled reaction that takes place in concert with a nucleation and growth mechanism.

Acknowledgments

The authors gratefully acknowledge the financial support of DOE/NREL High-Performance Photovoltaic Program, under subcontract No. XAT-4-33624-15. The authors also appreciate the sponsorship, in part, by the Assistant Secretary for Energy Efficiency and Renewable Energy, Office of FreedomCAR and Vehicle Technologies, as part of the High Temperature Materials Laboratory User Program, Oak Ridge National Laboratory, managed by UT-Battelle, LLC, for the U.S. Department of Energy under contract number DE-AC05-00OR22725.

References

- [1] M.A. Contreras, K. Ramanathan, J. AbuShama, F. Hasoon, D.L. Young, B. Egaas, R. Noufi, Prog. Photovolt: Res. Appl. 13 (2005) 209.
- [2] O. Schenker, M. Klenk, E. Bucher, Thin Solid Films 361–362 (2000) 454.

- [3] D. Fischer, N. Meyer, M. Kuczmik, M. Beck, A. Jäger-Waldau, M.Ch. Lux-Steiner, *Sol. Energy Mater. Sol. Cells* 67 (2001) 105.
- [4] M. Rusu, S. Wiesner, D.F. Marrón, A. Meeder, S. Doka, W. Bohne, S. Lindner, Th. Schedel-Niedrig, Ch. Giesen, M. Heuken, M.Ch. Lux-Steiner, *Thin Solid Films* 451–452 (2004) 556.
- [5] J.A. Abushama, S. Johnston, D. Young, R. Noufi, MRS Spring Meeting, CA, 2005.
- [6] A. Goetzberger, C. Hebling, H.-W. Schock, *Mater. Sci. Eng., R Rep.* 40 (2003) 1.
- [7] J. Palm, V. Probst, F.H. Karg, *Sol. Energy* 77 (6) (2004) 757.
- [8] S.N. Kundu, D. Bhattacharyya, S. Chaudhuri, A.K. Pal, *Mater. Chem. Phys.* 57 (3) (1999) 207.
- [9] R. Caballero, C. Guillén, *Sol. Energy Mater. Sol. Cells* 86 (2005) 1.
- [10] T. Gödecke, T. Haalboom, F. Ernst, *Z. Met.kd.* 91 (2000) 622.
- [11] T. Gödecke, T. Haalboom, F. Ernst, *Z. Met.kd.* 91 (2000) 635.
- [12] T. Gödecke, T. Haalboom, F. Ernst, *Z. Met.kd.* 91 (2000) 651.
- [13] S. Zweigart, D. Schmid, J. Kessler, H. Dittrich, H.W. Schock, *J. Cryst. Growth* 146 (1995) 233.
- [14] F.O. Adurodija, M.J. Carter, R. Hill, *Sol. Energy Mater. Sol. Cells* 37 (1995) 203.
- [15] A. Katsui, T. Iwata, *Thin Solid Films* 347 (1999) 151.
- [16] A. Brummer, V. Honkimaki, P. Berwian, V. Probst, J. Palm, R. Hock, *Thin Solid Films* 437 (2003) 297.
- [17] D. Wolf, G. Müller, *Thin Solid Films* 361–362 (2000) 155.
- [18] M. Purwins, A. Weber, P. Berwian, G. Müller, F. Hergert, S. Jost, R. Hock, *J. Cryst. Growth* 287 (2006) 408.
- [19] S. Kim, W.K. Kim, E.A. Payzant, R.M. Kaczynski, R.D. Acher, S. Yoon, T.J. Anderson, O.D. Crisalle, S.S. Li, *J. Vac. Sci. Technol., A, Vac. Surf. Films* 23 (2) (2005) 310.
- [20] W.K. Kim, S. Kim, E.A. Payzant, S.A. Speakman, S. Yoon, R.M. Kaczynski, R.D. Acher, T.J. Anderson, O.D. Crisalle, S.S. Li, V. Craciun, *J. Phys. Chem. Solids* 66 (11) (2005) 1915.
- [21] W.K. Kim, E.A. Payzant, S. Yoon, T.J. Anderson, *J. Cryst. Growth* 294 (2006) 231.
- [22] Y.S. Touloukian, R.K. Kirby, R.E. Taylor, P.D. Desai, *Thermophys. Prop. Matter* 12 (1977) 298.
- [23] T. Wada, N. Kohara, S. Nishiwaki, T. Negami, *Thin Solid Films* 387 (2001) 118.
- [24] W.N. Shafarman, J.E. Phillips, *Proceeding of 25th IEEE Photovoltaic Specialists Conference, Washington D.C., USA, May 13–17, 1996*, p. 917.
- [25] D. Abou-Ras, G. Kostorz, D. Bremaud, M. Kalin, F.V. Kurdesau, A.N. Tiwari, M. Dobeli, *Thin Solid Films* 480–481 (2005) 433.
- [26] F. Hulbert, *J. Br. Ceram. Soc.* 6 (1969) 11.